

# Elevated Carbon Dioxide Blunts Mammalian cAMP Signaling Dependent on Inositol 1,4,5-Triphosphate Receptor-mediated $\text{Ca}^{2+}$ Release<sup>\*[5]</sup>

Received for publication, February 15, 2012, and in revised form, May 15, 2012. Published, JBC Papers in Press, May 31, 2012, DOI 10.1074/jbc.M112.349191

Zara C. Cook<sup>‡§</sup>, Michael A. Gray<sup>¶</sup>, and Martin J. Cann<sup>‡§1</sup>

From the <sup>‡</sup>School of Biological and Biomedical Sciences and <sup>§</sup>Biophysical Sciences Institute, Durham University, South Road, Durham DH1 3LE, United Kingdom and <sup>¶</sup>Institute for Cell and Molecular Biosciences, The Medical School, Newcastle University, Framlington Place, Newcastle upon Tyne, NE2 4HH, United Kingdom

**Background:** Elevated  $\text{CO}_2$  is toxic to mammalian cells.

**Results:** Molecular  $\text{CO}_2$  reduces cellular cAMP dependent on intracellular  $\text{Ca}^{2+}$ .

**Conclusion:**  $\text{CO}_2$  can alter cellular physiological processes through  $\text{IP}_3$ -mediated  $\text{Ca}^{2+}$  release.

**Significance:** Altered  $\text{Ca}^{2+}$  signaling mediated by  $\text{CO}_2$  might underpin the detrimental effects of  $\text{CO}_2$  on the cell.

Elevated  $\text{CO}_2$  is generally detrimental to animal cells, suggesting an interaction with core processes in cell biology. We demonstrate that elevated  $\text{CO}_2$  blunts G protein-activated cAMP signaling. The effect of  $\text{CO}_2$  is independent of changes in intracellular and extracellular pH, independent of the mechanism used to activate the cAMP signaling pathway, and is independent of cell context. A combination of pharmacological and genetic tools demonstrated that the effect of elevated  $\text{CO}_2$  on cAMP levels required the activity of the  $\text{IP}_3$  receptor. Consistent with these findings,  $\text{CO}_2$  caused an increase in steady state cytoplasmic  $\text{Ca}^{2+}$  concentrations not observed in the absence of the  $\text{IP}_3$  receptor or under nonspecific acidotic conditions. We examined the well characterized cAMP-dependent inhibition of the isoform 3  $\text{Na}^+/\text{H}^+$  antiporter (NHE3) to demonstrate a functional relevance for  $\text{CO}_2$ -mediated reductions in cellular cAMP. Consistent with the cellular biochemistry, elevated  $\text{CO}_2$  abrogated the inhibitory effect of cAMP on NHE3 function via an  $\text{IP}_3$  receptor-dependent mechanism.

The importance of  $\text{CO}_2$  in biology is paramount.  $\text{CO}_2$  is integral to all life as the substrate for the  $\text{CO}_2$ -fixing enzyme ribulose 1,5-bisphosphate carboxylase/oxygenase (Rubisco)<sup>2</sup> in photosynthetic organisms and is a substrate/product for many other metabolic enzymes. The pH-dependent  $\text{CO}_2$ /bicarbonate equilibrium is fundamental to physiology and is intimately

associated with homeostatic mechanisms, including pH regulation, volume control, and fluid secretion.

All life on Earth has continued to flourish despite being subjected to large fluctuations in the levels of  $\text{CO}_2$  in both the atmosphere and aquatic environments (1). Photosynthetic organisms are able to acclimate to large changes in atmospheric  $\text{CO}_2$  (2). Fluctuations in  $\text{CO}_2$  can also apply stress to unicellular and multicellular organisms over much shorter time scales. Aquatic environments can show both diurnal and long-term seasonal variations in  $\text{CO}_2$  with consequent effects on photosynthetic organisms (3). Increased respiration during exercise can cause the partial pressure of  $\text{CO}_2$  rise from 35–45 mm Hg to over 120 mm Hg. Specific mechanisms exist to detect elevated  $\text{CO}_2$  and enable appropriate responses, but  $\text{CO}_2$  can also have relatively nonspecific deleterious effects on the cell (4).

$\text{CO}_2$  is proposed to enter cells through aquaporin, Amt, and Rhesus channels (5–7) and have direct effects on protein through carbamate formation, for example on Rubisco and hemoglobin (8). About 20 Protein Data Bank structures have  $\text{CO}_2$  as a ligand with a variety of modes of interaction but primarily through interactions with basic side chains (9).  $\text{CO}_2$  and  $\text{HCO}_3^-$  also influence a number of cell signaling processes.  $\text{CO}_2$  activates fungal pathogenesis through AC, and additional ACs from prokaryotes and mammals also respond directly to  $\text{CO}_2$  and  $\text{HCO}_3^-$  (10–12).  $\text{HCO}_3^-$  activates guanylyl cyclase types D and G to enable  $\text{CO}_2$  olfaction (13–15). The role of the cGMP pathway in  $\text{CO}_2$  chemosensing has also been conserved in *Caenorhabditis elegans* avoidance behavior (16–18). Chemosensing of  $\text{CO}_2$  in *Drosophila melanogaster* is mediated through *Gr21a* and *Gr63a*, two receptors of the seven-transmembrane domain class (19, 20). In mammals, ATP release is key to chemosensory control of respiration and increased  $\text{CO}_2$  permits ATP release from the medulla oblongata through a mechanism that requires connexin 26 (21, 22).  $\text{CO}_2$  is also chemosensed by specific taste receptor cells that express carbonic anhydrase type 4 and has evolutionarily conserved inhibitory effects on innate immunity through inhibition of NF- $\kappa$ B signaling (23–26). In acute acid-base disturbance, the proximal tubule cells of the mammalian kidney respond directly to  $\text{CO}_2$  to stimulate

\* This work was supported by Leverhulme Trust Grant F/00 128/AU, Biotechnology and Biological Sciences Research Council Grant BB/I011994/1, and Wellcome Trust Grant GR083381MA (to M. J. C.).

⚡ Author's Choice—Final version full access.

[5] This article contains supplemental Figs. S1–S3.

<sup>1</sup> To whom correspondence should be addressed: School of Biological and Biomedical Sciences, Biophysical Sciences Institute, Durham University, South Road, Durham DH1 3LE, UK. Tel.: 44-191-3343985; Fax: 44-191-3341201; E-mail: m.j.cann@durham.ac.uk.

<sup>2</sup> The abbreviations used are: Rubisco, ribulose 1,5-bisphosphate carboxylase/oxygenase; AC, adenylyl cyclase; 2-APB, 2-aminoethoxydiphenyl borate; Fsk, forskolin; Fura 2-AM, Fura-2 pentakis-acetoxymethyl ester;  $\text{IP}_3$ , inositol 1,4,5-triphosphate;  $\text{IP}_3\text{R}$ ,  $\text{IP}_3$  receptor; PTH, parathyroid hormone; BCECF-AM, 2',7'-bis(carboxyethyl)-5(6)-carboxyfluorescein acetoxymethyl ester; BAPTA-AM, 1,2-bis(2-aminophenoxy)ethane-*N,N,N',N'*-tetraacetic acid; OK, opossum kidney.

H<sup>+</sup> secretion through a mechanism involving a tyrosine kinase of the epidermal growth factor receptor family and intracellular Ca<sup>2+</sup> (27, 28). It is clear that specific mechanisms exist, through which CO<sub>2</sub> can interact with biological systems.

The examples provided are mechanisms by which CO<sub>2</sub> is detected specifically to initiate adaptive physiological responses, but CO<sub>2</sub> can have generally detrimental effects on animal cellular processes. In *C. elegans*, increased CO<sub>2</sub> causes slowed development, reduced fertility, and causes deterioration of body musculature (29). In *Drosophila*, elevated CO<sub>2</sub> causes defects in embryonic development and egg laying and hatching (25). Elevated CO<sub>2</sub> in rats stimulates renal phosphate excretion that is independent of other physiological factors, including pH (30). CO<sub>2</sub> will also impair alveolar fluid reabsorption in alveolar type II epithelial cells by inducing Na<sup>+</sup>, K<sup>+</sup>-ATPase endocytosis (31, 32). CO<sub>2</sub> can also chronically decrease cell proliferation through increasing levels of the miR-183 microRNA (33). Generally speaking, elevated CO<sub>2</sub> is tolerated in humans, although toxic effects on the central nervous system, cardiovascular, renal, metabolic, and respiratory systems are evident. Despite this, some individuals may show a greater sensitivity to the adverse effects of CO<sub>2</sub>, for example, in the presence of an increased intracranial pressure. The significance of this is that ventilation strategies in patients that induce hypercapnia, so-called "permissive hypercapnia," improves prognosis in models of acute lung injury, ischemia-reperfusion injury and acute respiratory distress syndrome (34, 35). The protective effect of permissive hypercapnia is explained to a large extent by the anti-inflammatory influence of CO<sub>2</sub>, but such immune suppression may be detrimental in clinical settings where infection or wounding is present (26, 36). There is a requirement, therefore, to understand the molecular basis of CO<sub>2</sub> interactions with the core processes of the cell to understand how CO<sub>2</sub> can be detrimental to cell function across the animal kingdom and also to inform clinical decisions regarding the use of permissive hypercapnia. In direct contrast to the current paradigm where CO<sub>2</sub> can activate specific physiological processes through accumulation of cyclic nucleotides, we demonstrate that CO<sub>2</sub> blunts cellular activities regulated by cAMP. This effect is independent of pH and requires Ca<sup>2+</sup> release via the IP<sub>3</sub> receptor. Given the ubiquity of cAMP and Ca<sup>2+</sup> signaling in mammalian cells, this work suggests a key mechanism by which CO<sub>2</sub> can have a broad spectrum of effects on cell physiology independent of pH.

### EXPERIMENTAL PROCEDURES

**Cell Culture**—OK cells (gift of Heini Murer, University of Zurich) and HEK-PR1 cells (gift of Colin Taylor, University of Cambridge) were cultured in Dulbecco's modified Eagle's medium (DMEM)/Ham's Nutrient Mixture F12 (1:1 volume), 15 mM HEPES, 14 mM NaHCO<sub>3</sub>, 10% (v/v) fetal bovine serum (FBS), 1% (v/v) penicillin-streptomycin, 2% (v/v) non-essential amino acids, 1% (v/v) L-glutamine, and 500 μg/ml G418 (HEK-PR1 cells only). UMR-106 cells (gift of James Gallagher, University of Liverpool) were cultured in DMEM, 15 mM HEPES, 14 mM NaHCO<sub>3</sub>, 10% (v/v) FBS, 1% (v/v) penicillin-streptomycin, 2% (v/v) non-essential amino acids, and 1% (v/v) L-glutamine. DT40KO and DT40-IP<sub>3</sub>R1 cells (gift of Colin Taylor) were cultured in RPMI 1640 medium, 15 mM HEPES, 14 mM NaHCO<sub>3</sub>,

10% (v/v) FBS, 1% (v/v) heat-inactivated chicken serum, 1% (v/v) penicillin-streptomycin, 2 mM glutamine, and 50 μM 2-mercaptoethanol.

**Measurement of Intracellular pH**—Cells attached to glass coverslips were loaded with 5 μM (HEK-PR1 cells) or 7.5 μM (OK cells) 2',7'-bis(carboxyethyl)-5(6)-carboxyfluorescein acetoxymethyl ester (BCECF-AM) for 30 min at 37 °C and 5% (v/v) CO<sub>2</sub>. pH<sub>i</sub> was measured using a microspectrofluorometric system (excitation, 490/440 nm; emission, 535 nm). pH<sub>i</sub> calibration was performed using high K<sup>+</sup> nigericin solutions (37).

**cAMP Accumulation**—Cells were starved overnight in 0.2% (w/v) BSA in serum-free medium and labeled for 2 h with 0.75 μCi ml<sup>-1</sup> [<sup>3</sup>H]adenine. Cells were washed with phosphate-buffered saline and incubated for 30 min at 37 °C at the desired CO<sub>2</sub> concentration in 990 μl of pre-incubation media (DMEM/F12 1:1 or DMEM depending on cell type, 15 mM HEPES, 1% (v/v) penicillin-streptomycin, 1 mM 3-isobutyl-1-methylxanthine) pre-gassed with the appropriate CO<sub>2</sub> concentration and with the pH adjusted. Assays were initiated with 10 μl of agonist. After 10 min at 37 °C, medium was removed, and cells were lysed with 1 ml 5% (w/v) trichloroacetic acid containing 1 mM ATP and 1 mM cAMP (OK, HEK-PR1, UMR-106 cells). cAMP was quantified by twin column chromatography (38). DT40KO and DT40-IP<sub>3</sub>R1 cell cAMP was assayed using the Biotrak cAMP enzyme immunoassay (GE Healthcare) according to the manufacturers instructions. Antagonists were added to the pre-incubation media.

**In Vitro Adenylyl Cyclase Assay**—Cell monolayers were washed with phosphate-buffered saline and suspended in lysis buffer (10 mM Tris-HCl, pH 7.5, 10 mM MgCl<sub>2</sub>, 5 mM CaCl<sub>2</sub>) for 20 min. The cell suspension was pelleted, re-suspended in lysis buffer, and incubated for a further 20 min. The cell suspension was pelleted and resuspended in 20 mM Tris-HCl, pH 7.5, 5 mM NaCl, 1 mM DTT, 1 mM 3-isobutyl-1-methylxanthine, 20% (v/v) glycerol, and homogenized through a 21-gauge needle. Adenylyl cyclase assays were performed at 37 °C in a final volume of 100 μl and contained 100 mM Tris-HCl, 100 mM NaCl, 1 mM DTT, 2 mM MgCl<sub>2</sub>, 1 mM 3-isobutyl-1-methylxanthine, 5 units of creatine phosphokinase, 5 μM creatine phosphate, and 1 mM [α<sup>32</sup>P]ATP (25 kBq). Reactions were stopped by the addition of 150 μl of 50 mM Tris-HCl, pH 7.5, 5% (w/v) SDS. A further 650 μl of H<sub>2</sub>O and 100 μl of 1 mM ATP, 1 mM [2,8-<sup>3</sup>H]cAMP (150 Bq) were added prior to separation of product [α<sup>32</sup>P]cAMP by the twin column method (38).

**Measurement of NHE3 Activity**—NHE3 activity was monitored by measuring pH<sub>i</sub> recovery after a NH<sub>4</sub>Cl pulse using BCECF-AM. OK cells were grown to 100% confluence on glass coverslips and starved overnight in 0.2% (v/v) BSA in serum-free media. 3-min NH<sub>4</sub>Cl pulses (110 mM NaCl, 25 mM glucose, 20 mM NH<sub>4</sub>Cl, 20 mM HEPES, 14 mM NaHCO<sub>3</sub>, 5 mM KCl, 1 mM CaCl<sub>2</sub>, 1 mM MgSO<sub>4</sub>, pH 7.4) were followed by at least 5 min of perfusion in the same solution with NaCl replacing NH<sub>4</sub>Cl.

**Ca<sup>2+</sup> Imaging**—Cells were loaded with 10 μM of the Ca<sup>2+</sup>-sensitive fluorescent dye Fura 2-AM in serum-free media for 30 min at 37 °C in 5% (v/v) CO<sub>2</sub> in air. Cells were washed and resuspended in Krebs-Ringer-HEPES solution (130 mM NaCl, 25 mM glucose, 20 mM HEPES, 14 mM NaHCO<sub>3</sub>, 5 mM KCl, 1 mM CaCl<sub>2</sub>, 1 mM MgSO<sub>4</sub>, pH 7.4) for 30 min at 37 °C in 5% (v/v)

CO<sub>2</sub> in air. CaCl<sub>2</sub> was omitted when examining the effect of extracellular Ca<sup>2+</sup>. Cells were transferred to fresh Krebs-Ringer-HEPES pre-gassed with the appropriate CO<sub>2</sub> concentration and the pH adjusted. Fura 2 emission was measured using a spectrofluorometer with simultaneous excitation at 340 and 380 nm and emission at 510 nm.

**Statistical Analysis**—Error bars represent the S.E. Statistical significance was determined by using Student's *t* test between indicated groups, unless otherwise indicated, and a 95% confidence interval was taken as *p* < 0.05.

## RESULTS

The study of the effects of molecular CO<sub>2</sub> *in vivo* are confused by delineating CO<sub>2</sub> effects from those due to the associated acidosis and in differentiating between CO<sub>2</sub> effects on the tissue of interest from those secondary to changes in the endocrine and autonomic nervous systems. As elevated CO<sub>2</sub> influences renal processes regulated by cAMP (39), we studied a renal proximal tubule-derived cell line (OK cells (40)) as a model to investigate the impact of CO<sub>2</sub> upon cAMP signaling. A previous study had revealed that elevated (10%) CO<sub>2</sub> had no apparent influence on cAMP accumulation but a drop in cAMP-response element-binding protein phosphorylation suggested that elevated CO<sub>2</sub> might be inhibitory for cAMP signaling (12). Methodology was therefore developed on the basis of this study to investigate the influence of elevated CO<sub>2</sub> on cAMP signaling.

PTH couples to the cAMP generating enzyme AC through its cognate receptor and the G protein subunit, G<sub>αs</sub>. cAMP accumulation in OK cells was reduced at 10% compared with 5% CO<sub>2</sub> at a PTH concentration (5 nM) of similar magnitude to that used for previous analysis of the influence of CO<sub>2</sub> on OK cell physiology (Fig. 1A) (41). Batch to batch variation is known to influence the sensitivity of OK cells to PTH (42), but the response to CO<sub>2</sub> was independent of cell batch or passage number. The reduction in cAMP was independent of extracellular pH, as reduction of the medium pH from 7.5 to 7.0 did not affect the response (Fig. 1B). The EC<sub>50</sub> for the response was unchanged as medium pH was dropped from 7.5 to 7.0 and cAMP accumulation actually increased (supplemental Fig. S1). The drop in cAMP in response to elevated CO<sub>2</sub> is therefore not explained by any potential acidification of medium pH on the assay. We measured final assay pH to assess whether changes in pH<sub>e</sub> at elevated CO<sub>2</sub> might still influence the observed response through an effect on the potency and efficacy of PTH stimulation of AC. Final assay pH<sub>e</sub> in assays performed at a starting pH<sub>e</sub> of 7.5 at 5% CO<sub>2</sub> was 7.5 ± 0.1 (mean ± S.D.) and at 10% CO<sub>2</sub> was 7.4 ± 0.1 (mean ± S.D.). The observed drop in cAMP accumulation, caused by elevated CO<sub>2</sub>, was therefore not unduly affected by any influence of pH<sub>e</sub> on signaling. cAMP levels were depressed by elevated CO<sub>2</sub> when AC was directly activated by 10 μM forskolin (FSK), indicating that the effect of CO<sub>2</sub> is independent of the mechanism used to stimulate AC (Fig. 1C). The FSK response was insensitive to a drop in medium pH from 7.5 to 7.0 (supplemental Fig. S2) indicating, together with the relative stability of assay pH at elevated CO<sub>2</sub>, that the response to CO<sub>2</sub> is not confused by any undue influence on pH<sub>e</sub>. To differentiate between effects of molecular CO<sub>2</sub> and effects due to intracellular pH (pH<sub>i</sub>), we examined the transient intracellular

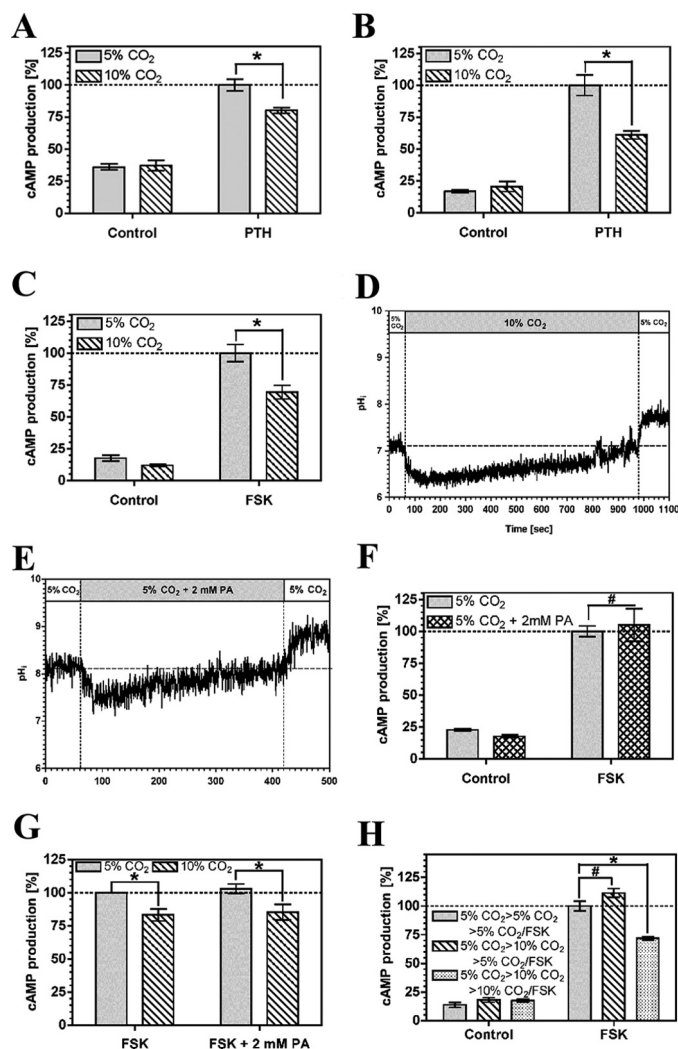
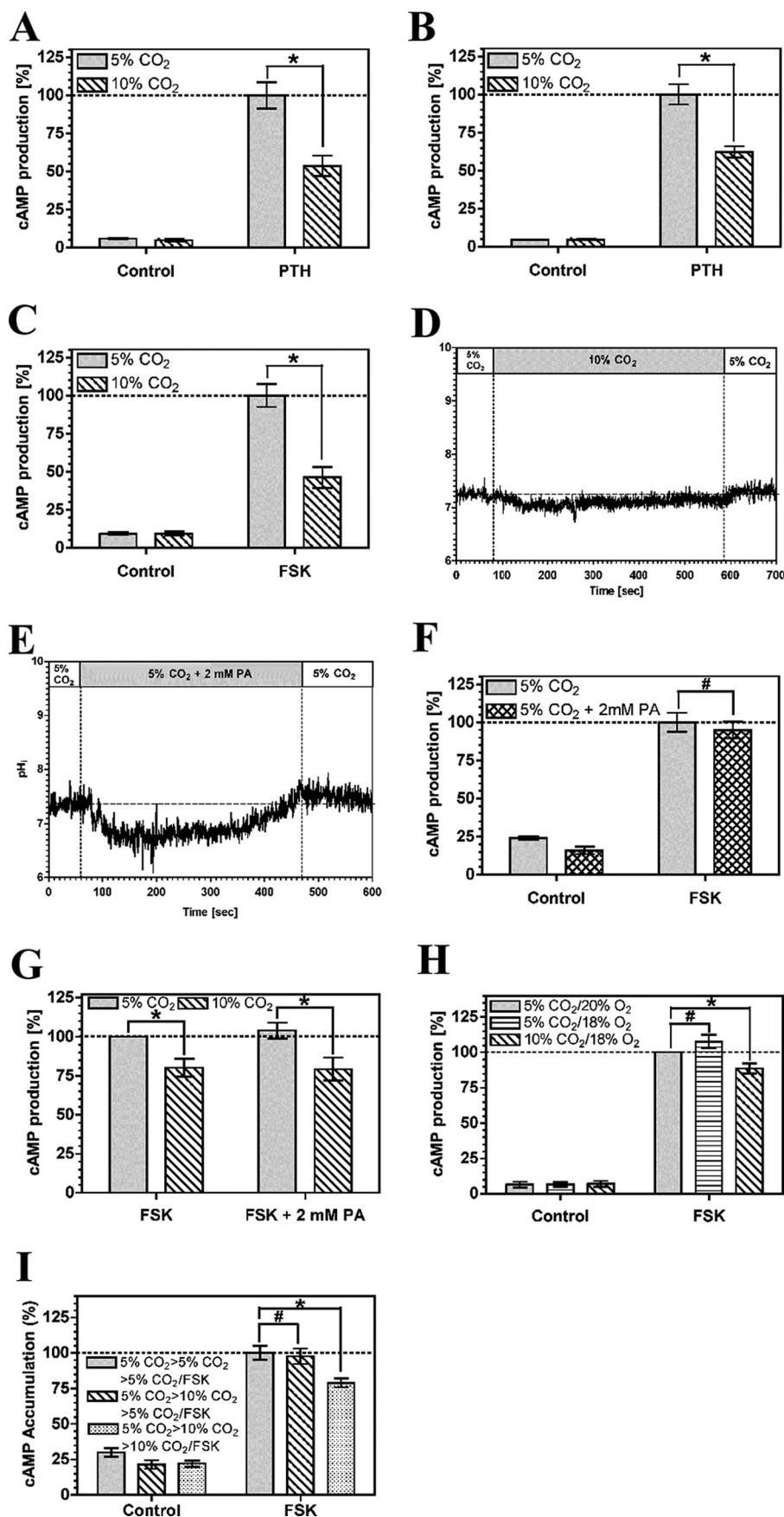


**FIGURE 1. Elevated CO<sub>2</sub> reduces cAMP accumulation in OK cells.** A, 5 nM PTH stimulated cAMP accumulation at 5% (v/v) CO<sub>2</sub> or 10% (v/v) CO<sub>2</sub> at pH 7.5. B, 5 nM PTH stimulated cAMP accumulation at 5% (v/v) CO<sub>2</sub> or 10% (v/v) CO<sub>2</sub> at pH 7.0. C, 10 μM FSK stimulated cAMP accumulation at 5% (v/v) CO<sub>2</sub> or 10% (v/v) CO<sub>2</sub> at pH 7.0. D, pH<sub>i</sub> in OK cells in response to elevated CO<sub>2</sub>. E, pH<sub>i</sub> in OK cells in response to 2 mM propionic acid (PA). F, 10 μM FSK stimulated cAMP accumulation at 5% (v/v) CO<sub>2</sub> with or without 2 mM propionic acid at pH 7.5. G, 10 μM FSK stimulated cAMP accumulation at 5% (v/v) CO<sub>2</sub> or 10% (v/v) CO<sub>2</sub> with 2 mM propionic acid at pH 7.5. H, OK cells at 5% (v/v) CO<sub>2</sub> were transferred to 5% (v/v) CO<sub>2</sub> or 10% (v/v) CO<sub>2</sub> for 30 min before assay at 5% (v/v) CO<sub>2</sub> or 10% (v/v) CO<sub>2</sub> with 10 μM FSK (pH 7.5). cAMP accumulation in each graph is normalized to the value in the presence of agonist at 5% (v/v) CO<sub>2</sub> (*n* > 3; \*, *p* < 0.05; #, not significant).

acidification caused by CO<sub>2</sub> (ΔpH<sub>i</sub> = −0.72 ± 0.17; Fig. 1D). We approximated the extent of intracellular acidification with media containing 2 mM propionic acid (ΔpH<sub>i</sub> = −0.60 ± 0.35; Fig. 1E). Transient intracellular acidification by propionic acid had no influence on cAMP indicating that the effect of CO<sub>2</sub> on cAMP is not mediated through pH<sub>i</sub> (Fig. 1F). Furthermore, propionic acid did not influence the response of cAMP to CO<sub>2</sub>, indicating that propionic acid does not influence the cAMP pathway such that it cannot respond to inhibitory signals (Fig. 1G). The effect of CO<sub>2</sub> on cAMP levels was fully reversible. Cells grown at 5% CO<sub>2</sub> and then exposed to 10% CO<sub>2</sub> prior to assay at 5% CO<sub>2</sub> with FSK demonstrated cAMP accumulation indistinguishable from cells maintained and assayed at 5% CO<sub>2</sub> (Fig. 1H). We examined whether the effect of CO<sub>2</sub> on AC activ-





ity was due to protein degradation. The *in vitro* AC activity of OK cell crude membrane preparations exposed to 5 or 10% CO<sub>2</sub> was similar (the specific activity at 10% CO<sub>2</sub> was  $115 \pm 8\%$  (S.E.,  $n = 6$ ) that at 5% CO<sub>2</sub>), indicating similar protein levels and consistent with the reversibility of the response to CO<sub>2</sub>.

To determine whether the CO<sub>2</sub> effect was cell context-specific, we examined the response of HEK 293 cells stably transfected with the human type 1 PTH receptor (HEK-PR1 cells) (43). cAMP accumulation stimulated by 5 nM PTH was reduced at elevated CO<sub>2</sub> independent of extracellular pH (Fig. 2, A and B, supplemental Fig. S1) and any specific pathway used to stimulate AC (10  $\mu$ M FSK; Fig. 2C and supplemental Fig. S2). 2 mM propionic acid gave a drop in pH<sub>i</sub> ( $\Delta$ pH<sub>i</sub> =  $-0.61 \pm 0.32$ ; Fig. 2E) greater than that for elevated CO<sub>2</sub> ( $\Delta$ pH<sub>i</sub> =  $-0.21 \pm 0.14$ ; Fig. 2D) but had no influence on cAMP accumulation (Fig. 2F). Similar to OK cells, propionic acid did not influence the response of cAMP to CO<sub>2</sub> (Fig. 2G). As the experimental process of elevating CO<sub>2</sub> in air causes a small hypoxic effect (from 19.9% to 18.9% O<sub>2</sub> (v/v)) we examined whether a shift from 20% to 18% O<sub>2</sub> at constant CO<sub>2</sub> influenced cAMP levels as an additional control. The mild hypoxia had no influence on cAMP indicating that the effect is mediated through CO<sub>2</sub> (Fig. 2H). Similar to OK cells, the *in vitro* AC activity of HEK-PR1 crude membrane preparations exposed to 5 or 10% CO<sub>2</sub> was similar (the specific activity at 10% CO<sub>2</sub> was  $99 \pm 5\%$  (S.E.,  $n = 5$ ) that at 5% CO<sub>2</sub>) indicating similar protein levels and cells grown at 5% CO<sub>2</sub> and then exposed to 10% CO<sub>2</sub> prior to assay at 5% CO<sub>2</sub> with FSK demonstrated cAMP accumulation indistinguishable from cells maintained and assayed at 5% CO<sub>2</sub> (Fig. 2I). To confirm that the effect of elevated CO<sub>2</sub> on cAMP is a broadly applicable phenomenon we also demonstrated that the PTH-responsive rat osteosarcoma cell line, UMR-106 (44), showed an identical response to CO<sub>2</sub> (supplemental Fig. S3).

The activity of the nine identified mammalian G protein-responsive AC isoforms can be modulated by a number of other signaling processes, and we investigated whether any of these pathways was responsible for the reduction in cAMP accumulation in response to CO<sub>2</sub>. We used antagonists whose broad target range enabled us to simultaneously inhibit multiple cAMP interacting signaling pathways (Fig. 3A). The effect of CO<sub>2</sub> on cAMP accumulation in HEK-PR1 cells did not require the activity of cAMP phosphodiesterase (1 mM 3-isobutyl-1-methylxanthine), soluble adenylyl cyclase (10  $\mu$ M KH7), cAMP-dependent protein kinase (PKA) (10  $\mu$ M H-89), calcium-calmodulin-dependent protein kinase II (100 nM autocamtide II), or protein kinase C (1  $\mu$ M staurosporine/1 mM Gö 6983). The lack of an effect of CO<sub>2</sub> with the AC inhibitor SQ 22,536 (200  $\mu$ M) demonstrated the requirement for a G protein-responsive AC (45) as opposed to soluble AC, which is unresponsive to SQ 22,536 (46, 47). Carbonic anhydrase inhibition (100  $\mu$ M acetazolamide) had no effect, indicating no requirement for conver-

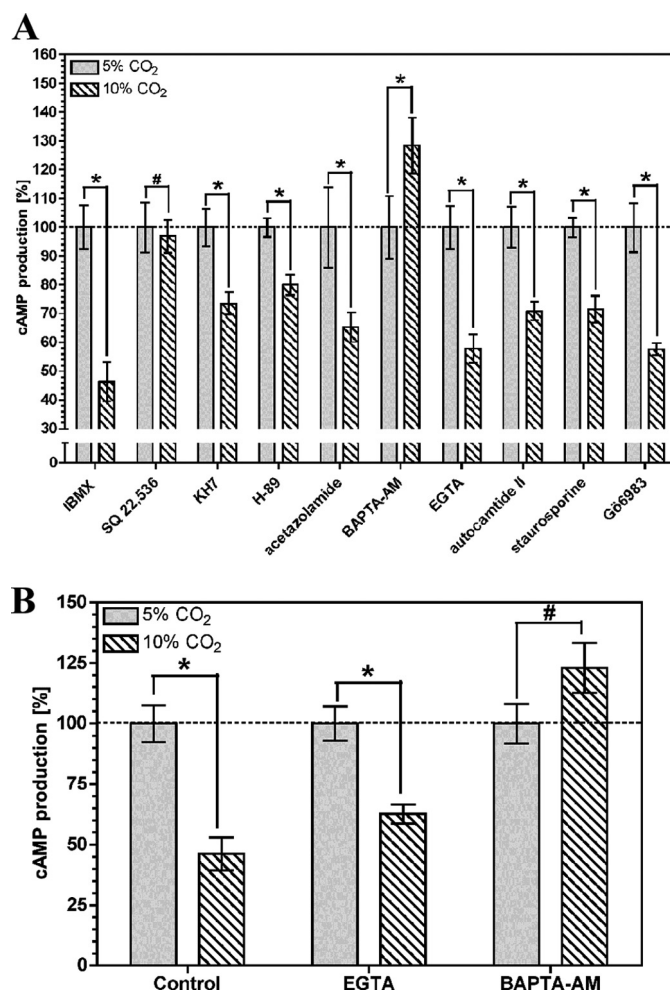


**FIGURE 3. Intracellular Ca<sup>2+</sup> is required for CO<sub>2</sub> to reduce cellular cAMP.** cAMP accumulation in HEK-PR1 (A) or OK cells (B) exposed to 5% (v/v) CO<sub>2</sub> or 10% (v/v) CO<sub>2</sub> at pH 7.5 in the presence of 10  $\mu$ M FSK and various antagonists. cAMP accumulation for each antagonist is normalized to the value at 5% (v/v) CO<sub>2</sub> ( $n > 4$ ; \*,  $p < 0.05$ ; #, not significant). IBMX, 3-isobutyl-1-methylxanthine.

sion of CO<sub>2</sub> to HCO<sub>3</sub><sup>-</sup> (14). 1 mM extracellular ethylene glycol tetraacetic acid (EGTA) had no effect on the CO<sub>2</sub> response, whereas it was ablated by the acetoxymethyl ester of 1,2-bis(2-aminophenoxy)ethane-*N,N,N',N'*-tetraacetic acid (BAPTA-AM; 1 mM), indicating a requirement for intracellular but not extracellular Ca<sup>2+</sup>. The influence of BAPTA-AM on the CO<sub>2</sub> response was confirmed in OK cells, demonstrating a likely common mechanism of action (Fig. 3B). We used further inhibitors to investigate the source of the intracellular Ca<sup>2+</sup>. The CO<sub>2</sub> effect was insensitive to 100  $\mu$ M nifedipine (L- and T-type voltage-dependent Ca<sup>2+</sup> channel blocker) in both OK and HEK-PR1 cells and 5  $\mu$ M rotenone (a mitochondrial inhibitor) in HEK-PR1 cells (Fig. 4, A and B). Rotenone ablated the response of cAMP to CO<sub>2</sub> in OK cells; however, we noted sig-

**FIGURE 2. Elevated CO<sub>2</sub> reduces cAMP accumulation in HEK-PR1 cells.** A, 5 nM PTH stimulated cAMP accumulation at 5% (v/v) CO<sub>2</sub> or 10% (v/v) CO<sub>2</sub> at pH 7.5. B, 5 nM PTH stimulated cAMP accumulation at 5% (v/v) CO<sub>2</sub> or 10% (v/v) CO<sub>2</sub> at pH 7.0. C, 10  $\mu$ M FSK stimulated cAMP accumulation at 5% (v/v) CO<sub>2</sub> or 10% (v/v) CO<sub>2</sub> at pH 7.0. D, pH<sub>i</sub> in HEK-PR1 cells in response to elevated CO<sub>2</sub>. E, pH<sub>i</sub> in HEK-PR1 cells in response to 2 mM propionic acid. F, 10  $\mu$ M FSK stimulated cAMP accumulation at 5% (v/v) CO<sub>2</sub> with or without 2 mM propionic acid at pH 7.5. G, 10  $\mu$ M FSK stimulated cAMP accumulation at 5% (v/v) CO<sub>2</sub> or 10% (v/v) CO<sub>2</sub> with 2 mM propionic acid (PA) at pH 7.5. H, 10  $\mu$ M FSK stimulated cAMP accumulation at 5% (v/v) CO<sub>2</sub>/20% (v/v) O<sub>2</sub>, 5% (v/v) CO<sub>2</sub>/18% (v/v) O<sub>2</sub>, or 10% (v/v) CO<sub>2</sub>/18% (v/v) O<sub>2</sub> at pH 7.5. I, HEK-PR1 cells at 5% (v/v) CO<sub>2</sub> were transferred to 5% (v/v) CO<sub>2</sub> or 10% (v/v) CO<sub>2</sub> for 30 min before assay at 5% (v/v) CO<sub>2</sub> or 10% (v/v) CO<sub>2</sub> with 10  $\mu$ M FSK (pH 7.5). cAMP accumulation in each graph is normalized to the value in the presence of agonist at 5% (v/v) CO<sub>2</sub> ( $n > 3$ ; \*  $p < 0.05$ ; #, not significant).

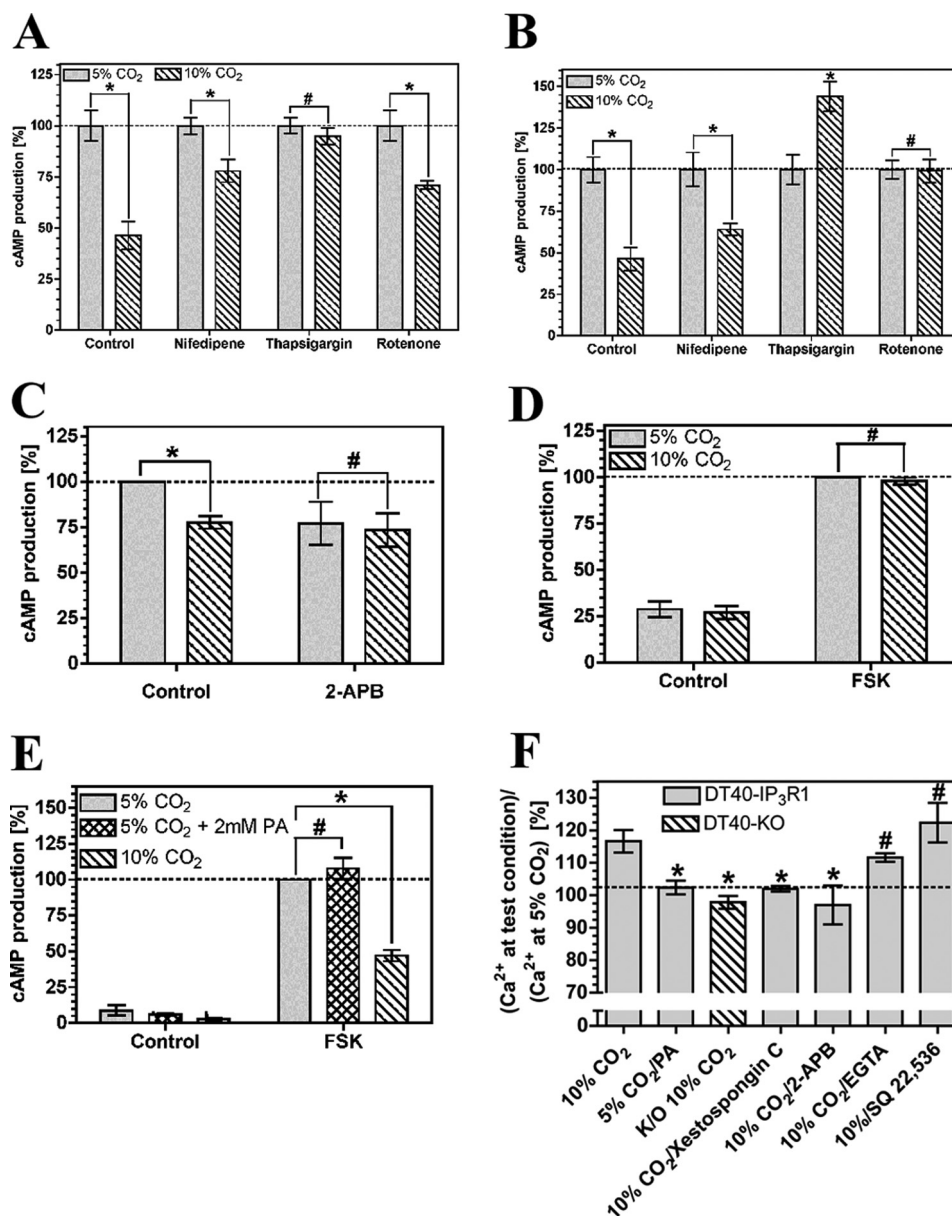
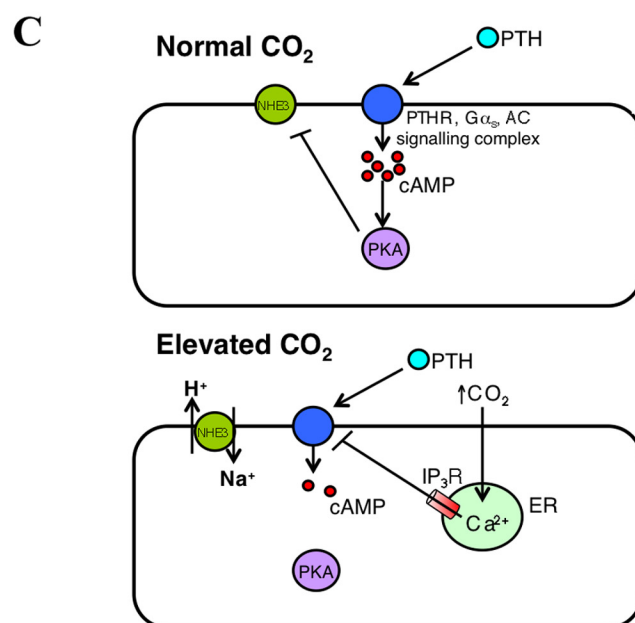
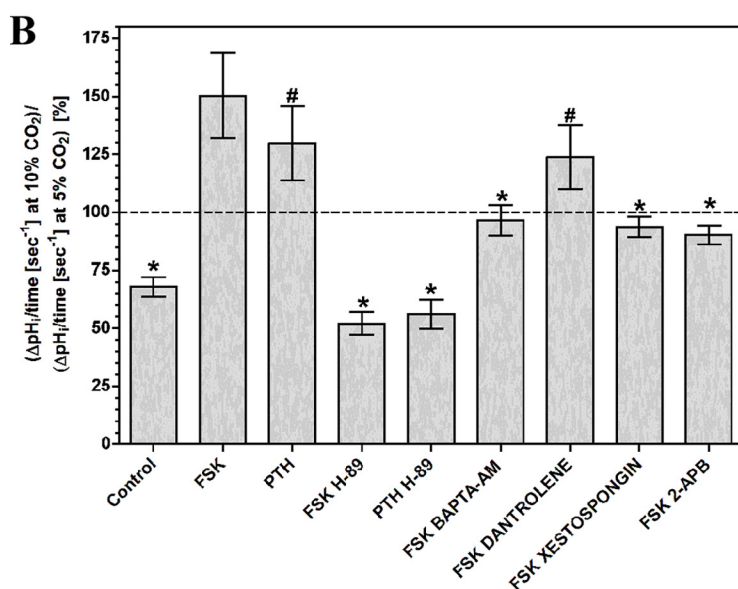
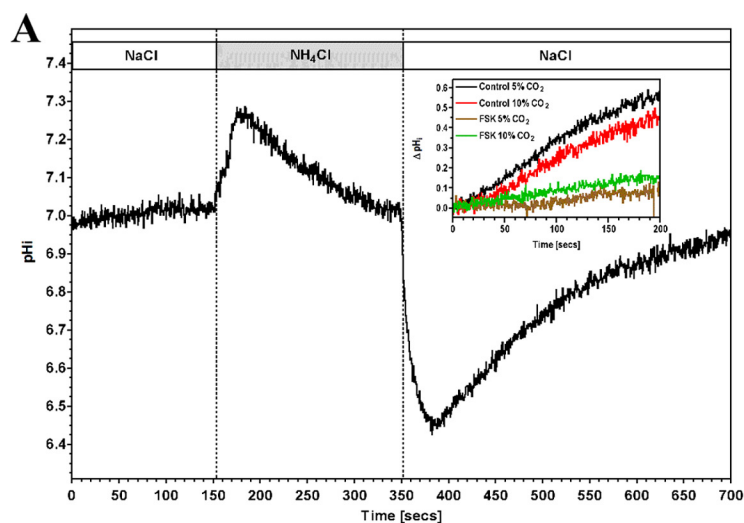


**FIGURE 4. Ca<sup>2+</sup> release via IP<sub>3</sub>R is required for CO<sub>2</sub> to reduce cellular cAMP.** A–C, cAMP accumulation in HEK-PR1 (A and C) or OK (B) cells exposed to 5% (v/v) CO<sub>2</sub> or 10% (v/v) CO<sub>2</sub> at pH 7.5 in the presence of 10  $\mu$ M FSK and various antagonists. cAMP accumulation for each antagonist is normalized to the value at 5% (v/v) CO<sub>2</sub> ( $n > 4$ ; \*,  $p < 0.05$ ; #, not significant). D and E, 10  $\mu$ M FSK stimulated cAMP accumulation in DT40KO (D), and DT40-IP<sub>3</sub>R1 cells (E) exposed to 5% (v/v) CO<sub>2</sub>, 10% (v/v) CO<sub>2</sub>, or 5% (v/v) CO<sub>2</sub> with 2 mM propionic acid (PA) at pH 7.5. cAMP accumulation in each graph is normalized to the value at 5% (v/v) CO<sub>2</sub> ( $n > 3$ ; \*,  $p < 0.05$ ; #, not significant). F, ratio of cytosolic Ca<sup>2+</sup> at a test condition versus 5% (v/v) CO<sub>2</sub> at pH 7.5 in DT40-IP<sub>3</sub>R1 or DT40-KO cells in the presence of various antagonists ( $n > 6$ ; \*,  $p < 0.05$ ; #, not significantly  $< 10\%$  (v/v) CO<sub>2</sub> by one-way analysis of variance with post-hoc one-sided Dunnett test).

nificant toxicity and cell death in response to rotenone in this cell line, indicating that this might be a nonspecific effect. The cAMP response was ablated by 10  $\mu$ M thapsigargin (endoplasmic reticulum Ca<sup>2+</sup>-ATPase inhibitor) in both HEK-PR1 and OK cells (Fig. 4, A and B). This indicated a likely role for CO<sub>2</sub> mediated Ca<sup>2+</sup> release from a thapsigargin-sensitive store, most likely via the IP<sub>3</sub> receptor and the endoplasmic reticulum. Further evidence for this was obtained in HEK-PR1 cells using the IP<sub>3</sub>R inhibitor 100  $\mu$ M 2-APB (Fig. 4C). To eliminate the possibility of off target effects with thapsigargin and 2-APB, particularly as significant variability was observed with the latter due to toxicity, we investigated more specific evidence for the involvement of the IP<sub>3</sub> receptor in Ca<sup>2+</sup> release. We exam-

ined the effect of elevated CO<sub>2</sub> on the DT40KO cell line (48). DT40KO cells are a chicken B lymphocyte-derived cell line genetically ablated for type 1, 2, and 3 IP<sub>3</sub> receptors and are a null background for IP<sub>3</sub> receptor studies. We examined cAMP accumulation in response to elevated CO<sub>2</sub> in DT40KO cells compared with DT40-IP<sub>3</sub>R1 cells that have had the rat IP<sub>3</sub> type 1 receptor introduced (49). Elevated CO<sub>2</sub> did not blunt cAMP accumulation in DT40KO cells (Fig. 4D) but did in DT40-IP<sub>3</sub>R1 cells (Fig. 4E), proving that the type 1 IP<sub>3</sub> receptor is required for the response to CO<sub>2</sub>. Intracellular acidification through 2 mM propionic acid had no influence on cellular cAMP in DT40-IP<sub>3</sub>R1 cells as observed for both OK and HEK-PR1 cells.





As the CO<sub>2</sub>/cAMP effect is sensitive to intracellular Ca<sup>2+</sup> chelation and shows a requirement for the IP<sub>3</sub> receptor, we investigated whether elevated CO<sub>2</sub> altered steady state cytoplasmic [Ca<sup>2+</sup>] in both DT40KO cells and DT40-IP<sub>3</sub>R1 cells. Cytoplasmic [Ca<sup>2+</sup>] was elevated at 10% compared with 5% CO<sub>2</sub> in DT40-IP<sub>3</sub>R1 but not DT40KO cells (Fig. 4F). Nonspecific intracellular acidification through propionic acid had no influence on cytoplasmic [Ca<sup>2+</sup>]. Elevated CO<sub>2</sub> therefore mediates Ca<sup>2+</sup> release from the endoplasmic reticulum via the IP<sub>3</sub> receptor. To provide an independent validation for the role of the IP<sub>3</sub> receptor in the DT40 cell response to CO<sub>2</sub>, we treated DT40-IP<sub>3</sub>R cells with either 1 mM EGTA, 100 μM 2-APB, or 500 nM xestospongine C (Fig. 4F). Cytoplasmic [Ca<sup>2+</sup>] was elevated at 10% compared with 5% CO<sub>2</sub> in DT40-IP<sub>3</sub>R1 cells in the presence of EGTA, consistent with the absence of an effect of EGTA on CO<sub>2</sub> modulation of cAMP. The Ca<sup>2+</sup> release in response to CO<sub>2</sub> was ablated by the IP<sub>3</sub> receptor antagonists xestospongine C and 2-APB. This result supports the interpretation that these inhibitors are blocking IP<sub>3</sub> receptor signaling in HEK-PR1 and OK cells (Figs. 4C and 5B). Inclusion of the AC inhibitor SQ 22,536 (200 μM) had no influence on CO<sub>2</sub>-mediated Ca<sup>2+</sup> release. These data confirm that an increase in cytosolic Ca<sup>2+</sup> is a prerequisite for the effect of CO<sub>2</sub> on cAMP (Fig. 4, D and E) and that cAMP lies downstream of the increase in cytosolic Ca<sup>2+</sup> (Fig. 4F).

We investigated the functional consequences of CO<sub>2</sub>-mediated reductions in intracellular cAMP by assessing a cAMP-dependent physiological process in OK cells. Sodium-proton exchanger isoform 3 (NHE3) is an apical Na<sup>+</sup>-H<sup>+</sup> antiporter of renal epithelial (and OK) cells with a crucial role in H<sup>+</sup>, Na<sup>+</sup>, and fluid homeostasis (50). NHE3 is inhibited by PKA phosphorylation at serine residues 552 and 605 (51), and we examined the effect of elevated CO<sub>2</sub> on cAMP-mediated suppression of NHE3 activity. OK cells exposed to NH<sub>4</sub>Cl alkalize due to H<sup>+</sup> buffering by NH<sub>3</sub>, but pH regulatory mechanisms returns pH<sub>i</sub> to normal (Fig. 5A). On exchange of NH<sub>4</sub>Cl for NaCl, pH<sub>i</sub> drops as the accumulated intracellular NH<sub>4</sub><sup>+</sup> releases H<sup>+</sup>. The alkalization to restore pH<sub>i</sub> is due to NHE3 (52), and we analyzed this phase of the response.

Comparison of control pH<sub>i</sub> recoveries at 5 and 10% CO<sub>2</sub> demonstrated a cAMP-independent suppression of recovery at elevated CO<sub>2</sub> (Fig. 5, A and B; note the ratio of recovery at 10% compared with 5% CO<sub>2</sub> < 1). Inhibition of NHE3-mediated pH<sub>i</sub> recovery by FSK or PTH was greater in 5% compared with 10% CO<sub>2</sub> consistent with the effect of CO<sub>2</sub> on cAMP levels (note the ratio of recovery at 10% CO<sub>2</sub> compared with 5% CO<sub>2</sub> > 1). The effect of CO<sub>2</sub> on cAMP inhibition of pH<sub>i</sub> recovery was reduced by H-89 and BAPTA-AM, demonstrating a requirement for both PKA and intracellular Ca<sup>2+</sup>. 10 μM dantrolene (a ryanodine receptor antagonist) had no influence on CO<sub>2</sub> suppression of cAMP signaling. The IP<sub>3</sub> receptor antagonists xestospongine C (500 nM) and 2-APB (100 μM) eliminated the effect of CO<sub>2</sub> on

cAMP-dependent NHE3 inhibition. CO<sub>2</sub> therefore suppresses the activity of the cAMP signaling pathway through Ca<sup>2+</sup> release via the IP<sub>3</sub> receptor with functional consequences for cAMP-dependent cellular processes (Fig. 5C).

## DISCUSSION

In this work, we make two original claims. The first is that molecular CO<sub>2</sub> reduces levels of cellular cAMP when the G-protein responsive cAMP signaling pathway is activated and this has functional consequences for downstream processes. This is in direct contrast to the current paradigm where cyclic nucleotide levels, where they are observed to respond to CO<sub>2</sub>, increase. The second is that molecular CO<sub>2</sub> increases steady state cytoplasmic Ca<sup>2+</sup> concentrations dependent on the IP<sub>3</sub> receptor. The effect of CO<sub>2</sub> on cAMP is a consequence of this altered Ca<sup>2+</sup>. These findings significantly advance our understanding of the effects of CO<sub>2</sub> on the cell.

CO<sub>2</sub> toxicity is not straightforward to study due to the effects of the associated acidosis and secondary effects on the endocrine and autonomic nervous systems. We circumvented these problems through the use of cultured cells to demonstrate that elevated CO<sub>2</sub> blunts cellular cAMP production independent of pH. The use of sub-maximally activating concentrations of cAMP stimulating agonists enabled us to detect either activation or down-regulation of the cAMP signaling pathway under any given experimental condition. Submaximal 5 nM PTH gave only a very small increase in cAMP in experiments to examine the influence of pH<sub>e</sub> in OK cells (supplemental Fig. S1). As the assay procedure used has minimal effects on pH<sub>e</sub>, this issue with this batch of cells does not affect the main findings. Cell batches used to examine the influence of CO<sub>2</sub> gave robust responses at submaximal 5 nM PTH (Figs. 1 and 5). In addition to a failure of intracellular acidification to modulate cAMP, two further lines of evidence make it unlikely that the effects of CO<sub>2</sub> are mediated by pH<sub>i</sub>. First, pH<sub>i</sub> is allowed to normalize after CO<sub>2</sub> elevation requiring a hypothesized acid signal to persist long after pH homeostasis. Second, FSK (activating all AC isoforms) and PTH (coupling to AC6 in HEKPR1 cells (53)) give identical responses to CO<sub>2</sub> arguing against a localized acid signal communicating with a distinct signaling enzyme. Extracellular pH is also unlikely to be responsible as medium acidification (as might be proposed to occur mid-assay were buffering insufficient) does not alter the EC<sub>50</sub> for PTH and actually gives an increase in cAMP. Medium acidification would therefore cause an underestimation of the decrease in cAMP. An increase in pCO<sub>2</sub> causes a small decrease in pO<sub>2</sub>, but the decrease in pO<sub>2</sub> did not explain the effects of pCO<sub>2</sub> on cAMP. We conclude, therefore, that the effect of hypercapnia is mediated by molecular CO<sub>2</sub> and not pH or any other variable.

The influence of CO<sub>2</sub> on cAMP signaling might be due to a direct interaction with AC or with an alternative signaling pathway, which impacts on cAMP levels. Pharmacological inhibi-

FIGURE 5. **Elevated CO<sub>2</sub> blunts cAMP inhibition of NHE3 in OK cells.** A, monitoring of pH<sub>i</sub> in OK cells in response to NH<sub>4</sub>Cl. The inset shows a sample experiment monitoring post-alkalization pH<sub>i</sub> recovery analyzed to generate the graph below. B, ratio of slope of pH<sub>i</sub> recovery at 10% (v/v) CO<sub>2</sub> versus 5% (v/v) CO<sub>2</sub> after shift from NH<sub>4</sub>Cl to NaCl in the presence of 10 μM FSK or 5 nM PTH and various inhibitors (*n* > 3; \*, *p* < 0.05; #, not significant compared with FSK by one-way analysis of variance with post-hoc Bonferroni test). C, model for the impact of CO<sub>2</sub> on PTH signaling at normal and elevated CO<sub>2</sub>. ER, endoplasmic reticulum.



tors offered the best initial route to investigate CO<sub>2</sub> responsive pathways that influence cAMP as the experiment could exploit the broad spectrum of targets antagonised under moderate concentrations. This method identified a role for intracellular Ca<sup>2+</sup> in the response to CO<sub>2</sub>. The Ca<sup>2+</sup> was most likely derived from an intracellular store as external EGTA did not influence the response. Further support came from the use of inhibitors previously used to study the role of Ca<sup>2+</sup> in cellular responses to CO<sub>2</sub> (27). Rotenone antagonized the cellular response to CO<sub>2</sub> in OK cells, but this is most likely due to its observed toxicity, particularly as the effect was not reproduced in HEK-PR1 cells. Thapsigargin ablated the cAMP response to CO<sub>2</sub> in both OK and HEK-PR1 cells. The use of 2-APB, which inhibits both the IP<sub>3</sub> receptor and transient receptor potential channels, supported this finding. The lack of a role for extracellular Ca<sup>2+</sup> eliminated the transient receptor potential channels and supported a role for Ca<sup>2+</sup> release from the endoplasmic reticulum, in particular via the IP<sub>3</sub> receptor. A role for the IP<sub>3</sub> receptor was proven through the use of a cell line genetically ablated for all three IP<sub>3</sub> receptor isoforms. The most likely interpretation of the pharmacological analysis in HEK-PR1 and OK cells is therefore supported unambiguously through genetics in an independent cell line. It is formally possible that the underlying signaling response to CO<sub>2</sub> in HEK-PR1 and OK cells does not involve the IP<sub>3</sub> receptor. This possibility is unlikely, however, as the IP<sub>3</sub> receptor antagonists used in this study were validated by demonstrating that their effect on CO<sub>2</sub>-mediated Ca<sup>2+</sup> release in DT40-IP<sub>3</sub>R1 cells was identical to the effect of the genetic ablation. A combination of the subtlety of the effects of CO<sub>2</sub> and the incomplete knockdown of the IP<sub>3</sub> receptor using siRNA (53) makes a genetic validation for the role of the IP<sub>3</sub> receptor in these cells currently unfeasible. Future experiments using knock-outs generated via zinc finger nucleases will permit a genetic approach to be adopted in these cells.

Despite this, a coherent picture does emerge and supports what is known of the toxicity of CO<sub>2</sub>. A role for altered Ca<sup>2+</sup> signaling in the response to CO<sub>2</sub> is consistent with generic toxicity as Ca<sup>2+</sup> signaling is a core physiological process evident in all mammalian cell types and elevated cytosolic Ca<sup>2+</sup> is associated with cell toxicity (54). The approximate 20% increase in steady state cytoplasmic Ca<sup>2+</sup> and 10–50% drop in cellular cAMP are relatively subtle effects and are consistent with the reasonable tolerance of mammals to elevated CO<sub>2</sub> (55). A role for Ca<sup>2+</sup> in CO<sub>2</sub> responses has been investigated previously. Vadász and co-workers (32) noted a transient increase in cytoplasmic Ca<sup>2+</sup> in response to hypercapnia, whereas Bouyer and co-workers (27) identified a rise in intracellular Ca<sup>2+</sup> proposed as originating from an unconventional source. Our work provides significant clarity in its use of genetics to identify the Ca<sup>2+</sup> source, but we cannot eliminate the possibility of context-dependent Ca<sup>2+</sup> sources. It will be instructive in the future to investigate whether the effects of Ca<sup>2+</sup> on AC are direct (56) or occur through a Ca<sup>2+</sup>-sensitive signaling pathway (57).

A crucial discovery is that elevated CO<sub>2</sub> suppresses a cAMP-dependent cellular process. The effect of CO<sub>2</sub> on a cAMP-responsive Na<sup>+</sup>-H<sup>+</sup> antiporter is consistent with the observed biochemistry of the influence of CO<sub>2</sub> on cAMP. We propose, therefore, that altered cAMP and/or Ca<sup>2+</sup> signaling can be

investigated further as a key mechanism by which the toxic effects of CO<sub>2</sub> are manifested. For example, there is growing evidence that chronic daytime hypercapnia associated with obstructive sleep disorders predisposes individuals to cardiovascular disease (58). The central role of cAMP and Ca<sup>2+</sup> in cardiac and circulatory physiology (57) suggests a key route to understanding this pathophysiology and possibilities for therapeutic intervention.

Ca<sup>2+</sup> efflux through the IP<sub>3</sub> receptor is modulated both by signaling pathways that regulate phospholipase C and by the local cellular environment (59–61). A major challenge for the future will be to determine how CO<sub>2</sub> causes Ca<sup>2+</sup> release through the IP<sub>3</sub> receptor and its direct cellular target. Identification of such a CO<sub>2</sub> target will further inform our understanding of the cell biology of CO<sub>2</sub>, in particular other cell processes that are influenced by CO<sub>2</sub> to mediate its toxicity.

*Acknowledgment—We thank Phil Townsend for helpful discussion and critical comments on the manuscript.*

## REFERENCES

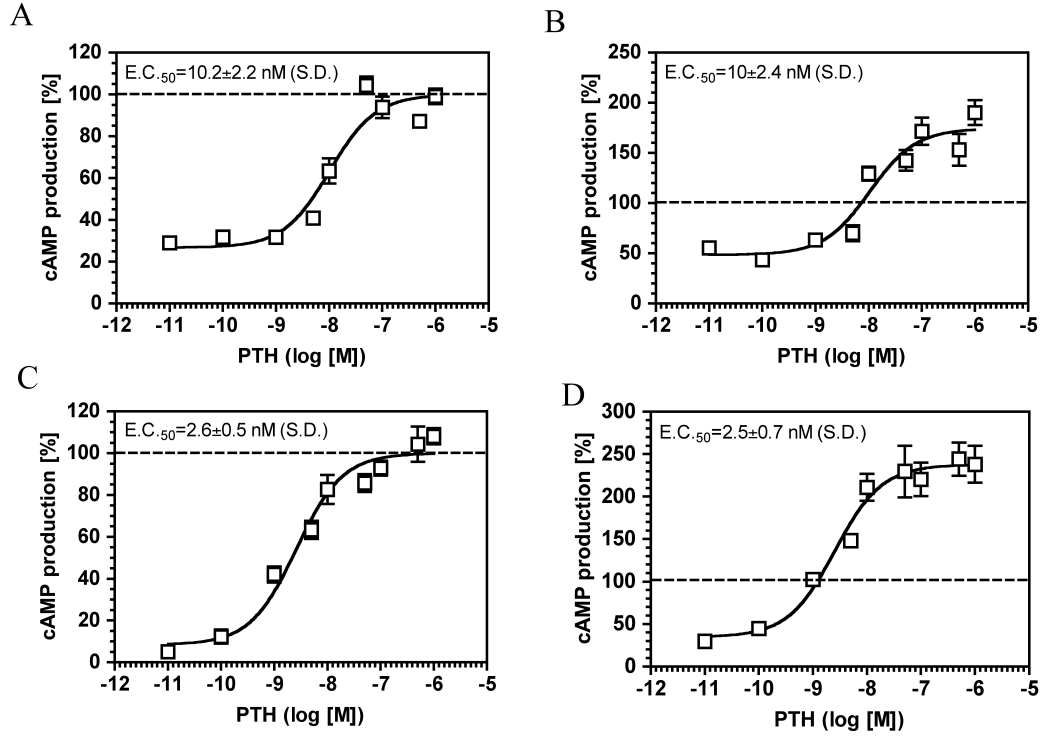
- Beerling, D. J., Lomax, B. H., Royer, D. L., Upchurch, G. R., Jr., and Kump, L. R. (2002) An atmospheric pCO<sub>2</sub> reconstruction across the Cretaceous-Tertiary boundary from leaf megafossils. *Proc. Natl. Acad. Sci. U.S.A.* **99**, 7836–7840
- Kaplan, A., Helman, Y., Tchernov, D., and Reinhold, L. (2001) Acclimation of photosynthetic microorganisms to changing ambient CO<sub>2</sub> concentration. *Proc. Natl. Acad. Sci. U.S.A.* **98**, 4817–4818
- Johnson, M. S., Billett, M. F., Dinsmore, K. J., Wallin, M., Dyson, K. E., and Jassal, R. S. (2010) Direct and continuous measurement of dissolved carbon dioxide in freshwater aquatic systems: Method and applications. *Ecology* **91**, 68–78
- Sharabi, K., Lecuona, E., Helenius, I. T., Beitel, G. J., Sznajder, J. I., and Gruenbaum, Y. (2009) Sensing, physiological effects, and molecular response to elevated CO<sub>2</sub> levels in eukaryotes. *J. Cell Mol. Med.* **13**, 4304–4318
- Soupe, E., Inwood, W., and Kustu, S. (2004) Lack of the Rhesus protein Rh1 impairs growth of the green alga *Chlamydomonas reinhardtii* at high CO<sub>2</sub>. *Proc. Natl. Acad. Sci. U.S.A.* **101**, 7787–7792
- Musa-Aziz, R., Chen, L. M., Pelletier, M. F., and Boron, W. F. (2009) Relative CO<sub>2</sub>/NH<sub>3</sub> selectivities of AQP1, AQP4, AQP5, AmtB, and RhAG. *Proc. Natl. Acad. Sci. U.S.A.* **106**, 5406–5411
- Nakhoul, N. L., Davis, B. A., Romero, M. F., and Boron, W. F. (1998) Effect of expressing the water channel aquaporin-1 on the CO<sub>2</sub> permeability of *Xenopus* oocytes. *Am. J. Physiol.* **274**, C543–548
- Lorimer, G. H. (1983) Carbon dioxide and carbamate formation: The makings of a biochemical control system. *Trends Biochem. Sci.* **8**, 65–68
- Cundari, T. R., Wilson, A. K., Drummond, M. L., Gonzalez, H. E., Jorgensen, K. R., Payne, S., Braunfeld, J., De Jesus, M., and Johnson, V. M. (2009) CO<sub>2</sub> Formatics: How do proteins bind carbon dioxide? *J. Chem. Inf. Model* **49**, 2111–2115
- Hammer, A., Hodgson, D. R., and Cann, M. J. (2006) Regulation of prokaryotic adenylyl cyclases by CO<sub>2</sub>. *Biochem. J.* **396**, 215–218
- Klengel, T., Liang, W. J., Chaloupka, J., Ruoff, C., Schröppel, K., Naglik, J. R., Eckert, S. E., Mogensen, E. G., Haynes, K., Tuite, M. F., Levin, L. R., Buck, J., and Mühlischlegel, F. A. (2005) Fungal adenylyl cyclase integrates CO<sub>2</sub> sensing with cAMP signaling and virulence. *Curr. Biol.* **15**, 2021–2026
- Townsend, P. D., Holliday, P. M., Fenik, S., Hess, K. C., Gray, M. A., Hodgson, D. R., and Cann, M. J. (2009) Stimulation of mammalian G-protein-responsive adenylyl cyclases by carbon dioxide. *J. Biol. Chem.* **284**, 784–791

13. Chao, Y. C., Cheng, C. J., Hsieh, H. T., Lin, C. C., Chen, C. C., and Yang, R. B. (2010) Guanylate cyclase-G, expressed in the Grueneberg ganglion olfactory subsystem, is activated by bicarbonate. *Biochem. J.* **432**, 267–273
14. Guo, D., Zhang, J. J., and Huang, X. Y. (2009) Stimulation of guanylyl cyclase-D by bicarbonate. *Biochemistry* **48**, 4417–4422
15. Sun, L., Wang, H., Hu, J., Han, J., Matsunami, H., and Luo, M. (2009) Guanylyl cyclase-D in the olfactory CO<sub>2</sub> neurons is activated by bicarbonate. *Proc. Natl. Acad. Sci. U.S.A.* **106**, 2041–2046
16. Bretscher, A. J., Busch, K. E., and de Bono, M. (2008) A carbon dioxide avoidance behavior is integrated with responses to ambient oxygen and food in *Caenorhabditis elegans*. *Proc. Natl. Acad. Sci. U.S.A.* **105**, 8044–8049
17. Hallem, E. A., Spencer, W. C., McWhirter, R. D., Zeller, G., Henz, S. R., Rättsch, G., Miller, D. M., 3rd, Horvitz, H. R., Sternberg, P. W., and Ringstad, N. (2011) Receptor-type guanylate cyclase is required for carbon dioxide sensation by *Caenorhabditis elegans*. *Proc. Natl. Acad. Sci. U.S.A.* **108**, 254–259
18. Hallem, E. A., and Sternberg, P. W. (2008) Acute carbon dioxide avoidance in *Caenorhabditis elegans*. *Proc. Natl. Acad. Sci. U.S.A.* **105**, 8038–8043
19. Jones, W. D., Cayirlioglu, P., Kadow, I. G., and Vosshall, L. B. (2007) Two chemosensory receptors together mediate carbon dioxide detection in *Drosophila*. *Nature* **445**, 86–90
20. Kwon, J. Y., Dahanukar, A., Weiss, L. A., and Carlson, J. R. (2007) The molecular basis of CO<sub>2</sub> reception in *Drosophila*. *Proc. Natl. Acad. Sci. U.S.A.* **104**, 3574–3578
21. Gourine, A. V., Llaudet, E., Dale, N., and Spyer, K. M. (2005) ATP is a mediator of chemosensory transduction in the central nervous system. *Nature* **436**, 108–111
22. Huckstepp, R. T., id Bihi, R., Eason, R., Spyer, K. M., Dicke, N., Willecke, K., Marina, N., Gourine, A. V., and Dale, N. (2010) Connexin hemichannel-mediated CO<sub>2</sub>-dependent release of ATP in the medulla oblongata contributes to central respiratory chemosensitivity. *J. Physiol.* **588**, 3901–3920
23. Chandrashekar, J., Yarmolinsky, D., von Buchholtz, L., Oka, Y., Sly, W., Ryba, N. J., and Zuker, C. S. (2009) The taste of carbonation. *Science* **326**, 443–445
24. Cummins, E. P., Oliver, K. M., Lenihan, C. R., Fitzpatrick, S. F., Bruning, U., Scholz, C. C., Slattery, C., Leonard, M. O., McLoughlin, P., and Taylor, C. T. (2010) NF- $\kappa$ B links CO<sub>2</sub> sensing to innate immunity and inflammation in mammalian cells. *J. Immunol.* **185**, 4439–4445
25. Helenius, I. T., Krupinski, T., Turnbull, D. W., Gruenbaum, Y., Silverman, N., Johnson, E. A., Sporn, P. H., Sznajder, J. I., and Beitel, G. J. (2009) Elevated CO<sub>2</sub> suppresses specific *Drosophila* innate immune responses and resistance to bacterial infection. *Proc. Natl. Acad. Sci. U.S.A.* **106**, 18710–18715
26. O'Toole, D., Hassett, P., Contreras, M., Higgins, B. D., McKeown, S. T., McAuley, D. F., O'Brien, T., and Laffey, J. G. (2009) Hypercapnic acidosis attenuates pulmonary epithelial wound repair by an NF- $\kappa$ B-dependent mechanism. *Thorax* **64**, 976–982
27. Bouyer, P., Zhou, Y., and Boron, W. F. (2003) An increase in intracellular calcium concentration that is induced by basolateral CO<sub>2</sub> in rabbit renal proximal tubule. *Am. J. Physiol. Renal Physiol.* **285**, F674–687
28. Zhou, Y., Bouyer, P., and Boron, W. F. (2006) Role of a tyrosine kinase in the CO<sub>2</sub>-induced stimulation of HCO<sub>3</sub><sup>-</sup> reabsorption by rabbit S2 proximal tubules. *Am. J. Physiol. Renal Physiol.* **291**, F358–367
29. Sharabi, K., Hurwitz, A., Simon, A. J., Beitel, G. J., Morimoto, R. I., Rechavi, G., Sznajder, J. I., and Gruenbaum, Y. (2009) Elevated CO<sub>2</sub> levels affect development, motility, and fertility and extend life span in *Caenorhabditis elegans*. *Proc. Natl. Acad. Sci. U.S.A.* **106**, 4024–4029
30. Guntupalli, J., Matthews, B., Carlin, B., and Bourke, E. (1987) Effect of acute hypercapnia on PTH-stimulated phosphaturia in dietary Pi-deprived rat. *Am. J. Physiol. Renal Physiol.* **253**, F34–40
31. Briva, A., Vadász, I., Lecuona, E., Welch, L. C., Chen, J., Dada, L. A., Trejo, H. E., Dumasius, V., Azzam, Z. S., Myrianthefs, P. M., Battle, D., Gruenbaum, Y., and Sznajder, J. I. (2007) High CO<sub>2</sub> levels impair alveolar epithelial function independently of pH. *PLoS ONE* **2**, e1238
32. Vadász, I., Dada, L. A., Briva, A., Trejo, H. E., Welch, L. C., Chen, J., Tóth, P. T., Lecuona, E., Witters, L. A., Schumacker, P. T., Chandel, N. S., Seeger, W., and Sznajder, J. I. (2008) AMP-activated protein kinase regulates CO<sub>2</sub>-induced alveolar epithelial dysfunction in rats and human cells by promoting Na<sub>2</sub>K-ATPase endocytosis. *J. Clin. Invest.* **118**, 752–762
33. Vohwinkel, C. U., Lecuona, E., Sun, H., Sommer, N., Vadász, I., Chandel, N. S., and Sznajder, J. I. (2011) Elevated CO<sub>2</sub> levels cause mitochondrial dysfunction and impair cell proliferation. *J. Biol. Chem.* **286**, 37067–37076
34. Laffey, J. G., and Kavanagh, B. P. (1999) Carbon dioxide and the critically ill—too little of a good thing? *Lancet* **354**, 1283–1286
35. Taylor, C. T., and Cummins, E. P. (2011) Regulation of gene expression by carbon dioxide. *J. Physiol.* **589**, 797–803
36. Nichol, A. D., O'Cronin, D. F., Howell, K., Naughton, F., O'Brien, S., Boylan, J., O'Connor, C., O'Toole, D., Laffey, J. G., and McLoughlin, P. (2009) Infection-induced lung injury is worsened after renal buffering of hypercapnic acidosis. *Crit. Care Med.* **37**, 2953–2961
37. Hegyi, P., Rakonczay, Z., Jr., Gray, M. A., and Argent, B. E. (2004) Measurement of intracellular pH in pancreatic duct cells: A new method for calibrating the fluorescence data. *Pancreas* **28**, 427–434
38. Salomon, Y., Londos, C., and Rodbell, M. (1974) A highly sensitive adenylyl cyclase assay. *Anal. Biochem.* **58**, 541–548
39. Guntupalli, J., and Bourke, E. (1985) Evidence that the phosphaturic effect of acute hypercapnia (HC) is not due to the low systemic pH of HC. *Kidney Int.* **27**, 116
40. Koyama, H., Goodpasture, C., Miller, M. M., Teplitz, R. L., and Riggs, A. D. (1978) Establishment and characterization of a cell line from the American opossum (*Didelphys virginiana*). *In Vitro* **14**, 239–246
41. Jehle, A. W., Hilfiker, H., Pfister, M. F., Biber, J., Lederer, E., Krapf, R., and Murer, H. (1999) Type II Na-Pi cotransport is regulated transcriptionally by ambient bicarbonate/carbon dioxide tension in OK cells. *Am. J. Physiol.* **276**, F46–53
42. Cole, J. A., Forte, L. R., Krause, W. J., and Thorne, P. K. (1989) Clonal sublines that are morphologically and functionally distinct from parental OK cells. *Am. J. Physiol.* **256**, F672–679
43. Short, A. D., and Taylor, C. W. (2000) Parathyroid hormone controls the size of the intracellular Ca<sup>2+</sup> stores available to receptors linked to inositol trisphosphate formation. *J. Biol. Chem.* **275**, 1807–1813
44. Martin, T. J., Ingleton, P. M., Underwood, J. C., Michelangeli, V. P., Hunt, N. H., and Melick, R. A. (1976) Parathyroid hormone-responsive adenylyl cyclase in induced transplantable osteogenic rat sarcoma. *Nature* **260**, 436–438
45. Hurley, J. H. (1999) Structure, mechanism, and regulation of mammalian adenylyl cyclase. *J. Biol. Chem.* **274**, 7599–7602
46. Spehr, M., Schwane, K., Riffell, J. A., Barbour, J., Zimmer, R. K., Neuhaus, E. M., and Hatt, H. (2004) Particulate adenylyl cyclase plays a key role in human sperm olfactory receptor-mediated chemotaxis. *J. Biol. Chem.* **279**, 40194–40203
47. Leclerc, P., and Kopf, G. S. (1999) Evidence for the role of heterotrimeric guanine nucleotide-binding regulatory proteins in the regulation of the mouse sperm adenylyl cyclase by the egg's zona pellucida. *J. Androl.* **20**, 126–134
48. Sugawara, H., Kurosaki, M., Takata, M., and Kurosaki, T. (1997) Genetic evidence for involvement of type 1, type 2, and type 3 inositol 1,4,5-trisphosphate receptors in signal transduction through the B-cell antigen receptor. *EMBO J.* **16**, 3078–3088
49. Laude, A. J., Tovey, S. C., Dedos, S. G., Potter, B. V., Lummis, S. C., and Taylor, C. W. (2005) Rapid functional assays of recombinant IP<sub>3</sub> receptors. *Cell Calcium* **38**, 45–51
50. Alexander, R. T., and Grinstein, S. (2009) Tethering, recycling, and activation of the epithelial sodium-proton exchanger, NHE3. *J. Exp. Biol.* **212**, 1630–1637
51. Zhao, H., Wiederkehr, M. R., Fan, L., Collazo, R. L., Crowder, L. A., and Moe, O. W. (1999) Acute inhibition of Na/H exchanger NHE-3 by cAMP. Role of protein kinase A and NHE-3 phosphoserines 552 and 605. *J. Biol. Chem.* **274**, 3978–3987
52. Weinman, E. J., Steplock, D., Wade, J. B., and Shenolikar, S. (2001) Ezrin binding domain-deficient NHERF attenuates cAMP-mediated inhibition of Na<sup>+</sup>/H<sup>+</sup> exchange in OK cells. *Am. J. Physiol. Renal Physiol.* **281**, F374–380
53. Tovey, S. C., Dedos, S. G., Taylor, E. J., Church, J. E., and Taylor, C. W.

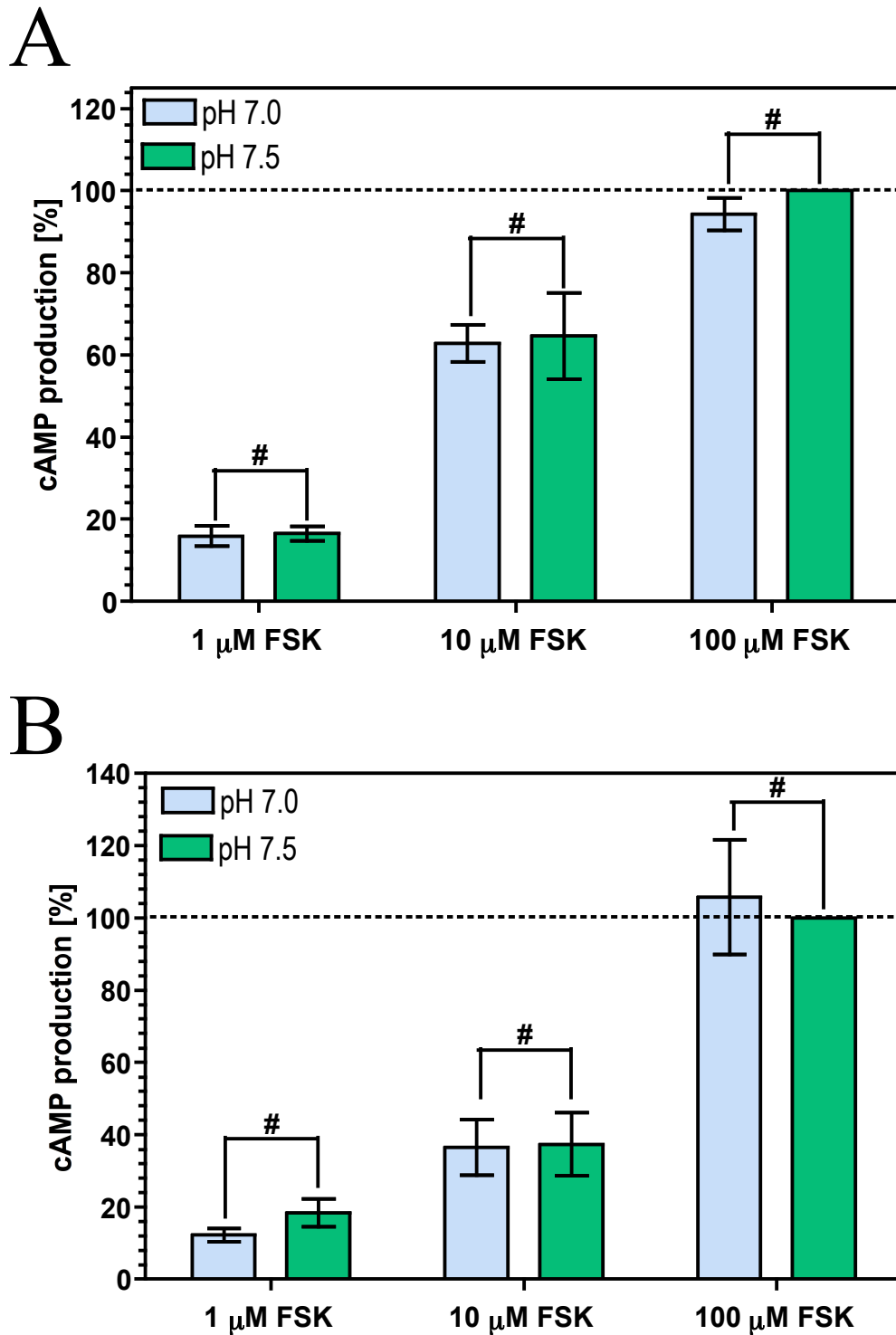
- (2008) Selective coupling of type 6 adenylyl cyclase with type 2 IP<sub>3</sub> receptors mediates direct sensitization of IP<sub>3</sub> receptors by cAMP. *J. Cell Biol.* **183**, 297–311
54. Johnson, M. E., Gores, G. J., Uhl, C. B., and Sill, J. C. (1994) Cytosolic free calcium and cell death during metabolic inhibition in a neuronal cell line. *J. Neurosci.* **14**, 4040–4049
  55. Adrogué, H. E., and Adrogué, H. J. (2001) Acid-base physiology. *Respir. Care* **46**, 328–341
  56. Mou, T. C., Masada, N., Cooper, D. M., and Sprang, S. R. (2009) Structural basis for inhibition of mammalian adenylyl cyclase by calcium. *Biochemistry* **48**, 3387–3397
  57. Willoughby, D., and Cooper, D. M. (2007) Organization and Ca<sup>2+</sup> regulation of adenylyl cyclases in cAMP microdomains. *Physiol. Rev.* **87**, 965–1010
  58. Gopalakrishnan, P., and Tak, T. (2011) Obstructive sleep apnea and cardiovascular disease. *Cardiol. Rev.* **19**, 279–290
  59. Rossi, A. M., Tovey, S. C., Rahman, T., Prole, D. L., and Taylor, C. W. (2011) *Biochim. Biophys. Acta* [Epub ahead of print]
  60. Li, G., Mongillo, M., Chin, K. T., Harding, H., Ron, D., Marks, A. R., and Tabas, I. (2009) Role of ERO1- $\alpha$ -mediated stimulation of inositol 1,4,5-triphosphate receptor activity in endoplasmic reticulum stress-induced apoptosis. *J. Cell Biol.* **186**, 783–792
  61. Higo, T., Hattori, M., Nakamura, T., Natsume, T., Michikawa, T., and Mikoshiba, K. (2005) Subtype-specific and ER lumenal environment-dependent regulation of inositol 1,4,5-trisphosphate receptor type 1 by ERp44. *Cell* **120**, 85–98



**Supplementary Figure 1.** Extracellular pH does not influence the potency of the PTH receptor-AC signalling complex for PTH. cAMP accumulation in OK (A, B) or HEK-PR1 cells (C, D) at pH 7.5 (A, C) or pH 7.0 (B, D) at varying PTH. cAMP accumulation in each cell line is normalized to the value for the best fit for maximum cAMP accumulation at pH 7.5 ( $n > 4$ ).



**Supplementary Figure 2.** Extracellular pH does not influence the efficacy or potency of the forskolin mediated cAMP response. cAMP accumulation in OK ( $n = 4$ , # not significant) (A) or HEK-PR1 cells ( $n = 3$ , # not significant) (B) at pH 7.0 or 7.5 at varying forskolin (FSK). cAMP accumulation in each cell line is normalized to the response to 100  $\mu$ M forskolin at pH 7.5.



**Supplementary Figure 3.** Elevated CO<sub>2</sub> reduces cAMP accumulation in UMR-106 cells. cAMP accumulation in UMR-106 cells exposed to 5% (v/v) CO<sub>2</sub> or 10% (v/v) CO<sub>2</sub> at pH 7.5 (A, C) and pH 7.0 (B, D) in the presence of 5 nM PTH (A, B) or 10  $\mu$ M FSK (C, D). cAMP accumulation in each graph is normalized to the value in the presence of agonist at 5% (v/v) CO<sub>2</sub> ( $n > 4$ , \*  $p < 0.05$ ).

